



## Modelling Low Velocity Zones in Box Culverts to Assist Fish Passage

X. Leng<sup>1</sup> and H. Chanson<sup>1</sup>

<sup>1</sup>The University of Queensland, School of Civil Engineering, Brisbane 4072, Australia

### Abstract

A culvert is a covered channel designed to pass water through an embankment. The recognition of the adverse ecological impacts of culverts on upstream fish passage is driving the development of new culvert design guidelines, with a focus on small-bodied fish species seeking low velocity zones (LVZs) to minimise energy expenditure. Herein a hybrid modelling technique was applied, combining physical modelling, one-dimensional numerical modelling and three-dimensional computational fluid dynamics modelling (3D CFD). The results reveal fundamental turbulent processes that may affect small fish navigability and provide new insights for the development of standard box culvert design guidelines.

### Introduction

A culvert is a relatively short covered channel designed to pass water as an open channel flow through an embankment (Henderson 1966, Apelt 1983) (Fig. 1a). The optimum engineering designs of culvert typically require the smallest barrel size compatible with an inlet control operation at design flow conditions (Herr and Bossy 1965, Chanson 2000,2004). The barrel is the narrowest section beneath the embankment (Fig. 1b). The resulting design leads to excessive barrel velocities for design and less-than-design discharges, with adverse impact on upstream fish passage (Behlke et al. 1991, Warren and Pardew 1998, Olsen and Tullis 2013). The recognition of the ecological impacts of culverts as fish barriers is driving the development of new culvert design guidelines, with a particular focus on small-body-mass fish in Australia (Fairfull and Whitheridge 2003, Moore et al. 2018). Fish behaviour is closely linked to the surrounding turbulent flow environment. A targeted fish species may react to the local turbulence patterns and secondary flow motions during upstream fish passage, seeking low velocity zones (LVZs) to minimise its energy expenditure (Wang et al. 2016, Wang and Chanson 2018). In some application, baffles and boundary roughening may be installed along the culvert barrel invert to decrease the flow velocity, but the additional flow resistance can reduce drastically the culvert discharge capacity for a given afflux (Quadrio 2007, Olsen and Tullis 2013).

In the present study, a hybrid modelling technique was applied, combining physical modelling, depth-averaged numerical modelling and three-dimensional computational fluid dynamics modelling (3D CFD) of a standard box culvert barrel. Detailed CFD validation was undertaken against laboratory studies obtained under carefully controlled flow conditions. This study focuses on the upstream passage of small-bodied native species in Australia, with initial tests undertaken with juvenile silver perch (*Bidyanus bidyanus*) and Duboulay's rainbowfish (*Melanotaenia duboulayi*) in a 12 m long 0.5 m wide culvert barrel channel (Wang et al. 2016, Cabonce et al. 2018).

### Methodology

Flow through a standard box culvert barrel was modelled using hybrid technique, consisting of experimental, one-dimensional reduced model, and numerical CFD simulation. Physical modelling was performed in two facilities: a

complete box culvert model and a 12 m long 0.5 m wide culvert barrel flume (Figs. 1b & 1c). The culvert model was located in a 1 m wide flume. The barrel was 0.50 m long, 0.150 m wide and 0.105 m high. Its design discharge was  $Q_{des} = 0.010 \text{ m}^3/\text{s}$  for a maximum acceptable afflux of 0.087 m. The culvert barrel flume was 12 m long and 0.50 m wide, typical of a full-scale single-cell culvert structure beneath a two-lane road in eastern Australia. The water discharges were measured with sharp-edge orifice meters calibrated in-situ, with an accuracy of 2%. The water depths were measured with pointer gauges within  $\pm 0.0005 \text{ m}$ . Water velocities were recorded with Prandtl-Pitot tube and acoustic Doppler velocimetry, while the boundary shear stress was measured with a carefully-calibrated Preston tube (Cabonce et al. 2018).

CFD modelling was conducted with Ansys<sup>TM</sup> Fluent v. 18.0, on a Dell<sup>TM</sup> Precision T5810 workstation (Xeon<sup>®</sup> E5-1680v4 processor, 128 Gb RAM). The numerical model solves the governing continuity and momentum equations for a steady, incompressible flow:

$$\frac{\partial V_i}{\partial x_i} = 0 \quad (1)$$

$$\frac{\partial V_i}{\partial t} + V_j \times \frac{\partial V_i}{\partial x_j} = g_i - \frac{1}{\rho} \times \frac{\partial P}{\partial x_i} + \frac{\partial \tau_{ij}}{\partial x_j} \quad (2)$$

where  $V_i$  is the velocity component in the direction  $x_i$  ( $x_i = x, y, z$ ),  $t$  is the time,  $g_i$  is the gravity component in the direction  $x_i$ ,  $\rho$  is the fluid density,  $P$  is the pressure, and  $\tau_{ij}$  is the shear stress tensor component of the  $i$ -momentum transported in the  $j$ -direction (Liggett 1994). The free-surface is tracked using the Volume of Fluid (VoF) method (Hirt and Nichols 1981).

One dimensional (1D) numerical modelling was based upon the differential form of the energy equation for open channel flow, called the backwater equation (Henderson 1966). Calculations were performed using the standard step method, starting from the outlet conditions.

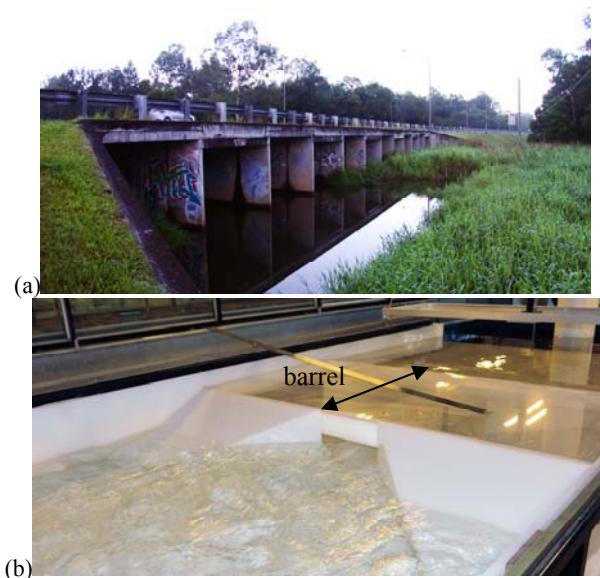




Figure 1. Standard box culvert modelling. (a) Prototype box culvert inlet beneath Paradise Road, Logan QLD. (b) Complete box culvert model ( $B = 0.15$  m). (c) Culvert barrel model (barrel width  $B = 0.5$  m).

### Numerical method and model configuration

The test culvert was modelled as a rectangular prismatic channel with zero bed slope and smooth walls. The culvert barrel was 8 m long, 0.5 m wide and 0.5 m high, with an extruded inlet being 0.2 m long, 0.2 high, and 0.5 m wide. It was configured as a velocity inlet, and the inflow discharge was  $0.056 \text{ m}^3/\text{s}$ . The inflow discharge was selected based upon the experimental study of Cabonce et al (2017,2018), to achieve systematic validation with experimental data. The outlet was configured as a pressure outlet, with a specified tailwater depth  $d_{\text{out}} = 0.16$  m according to the experimental data. In the field, a tailwater level is the natural water level observed at the downstream flood plain. Figure 1 illustrates the numerical domain. The boundary conditions are colour-coded, and detailed in Table 1.

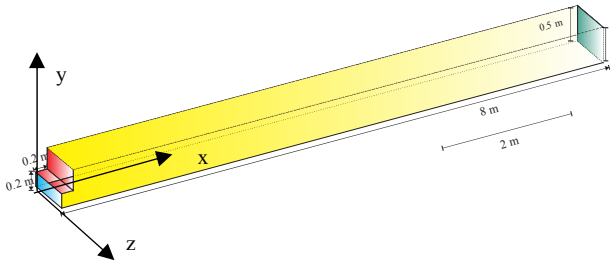


Figure 2. Three-dimensional (3D) sketch of numerical domain with colour-coded boundaries; detailed boundary conditions corresponding to each colour listed in Table 1.

Colour	Boundary condition	Remarks
Blue	Velocity inlet	$V_{\text{in}} = 0.56 \text{ m/s}$
Red	Symmetry <sup>(1)</sup>	--
Yellow	Wall	Roughness = 0 Uniform roughness
Green	Pressure outlet	$d_{\text{out}} = 0.16 \text{ m}$

Table 1. Colour-coding of boundary conditions (see Figure 2).

The numerical CFD study consisted of two stages of modelling: (1) transient flow simulation in a 3D culvert channel with coarse mesh; the coarse mesh consisted of uniform squares with 0.1 m grid size throughout the numerical domain; and (2) transient flow simulation in a 3D culvert channel with refined mesh; the mesh was refined into non-uniform gradually varied squares using a bias function:

<sup>1</sup> Symmetry conditions were used for the two boundaries adjacent to the inlet. The two boundaries acted as slip walls which gave more flexibility in changing the height and velocity of the inlet flow, with negligible impact to the water flow field further downstream.

$$L = \sum_0^i L_1 \times r^i \quad (3)$$

where  $L$  is the size of the meshed edge,  $L_1$  is the size of the first element calculated using a bias factor  $bf$ ,  $r$  is the growth rate,  $n$  is the number of division specified and  $i = 1, 2, 3, \dots, n-1$ . The relationship between growth factor  $r$  and bias factor  $bf$  is:

$$bf = r^{(n-1)} \quad (4)$$

Biased mesh with refinement near the walls and sidewalls were essential to simulate realistic flow patterns near the boundaries. The smallest grid size in the vertical direction was  $\Delta y_{\text{min}} = 0.001$  m with a growth factor of 1.12. The smallest grid size in the transverse direction was  $\Delta z_{\text{min}} = 0.002$  m with a growth factor of 1.17. The mesh in the stream-wise  $x$  direction was uniformly partitioned with a grid size  $\Delta x = 0.1$  m.

All models used a  $k-\epsilon$  method to solve the turbulent terms in the Navier-Stokes equations. The transient formulation was solved implicitly with a second order upwind scheme for momentum, first order upwind scheme for turbulent kinetic energy and turbulent dissipation rate. The convergence was ensured by reducing residuals of all parameters to  $10^{-4}$  or less. All simulations were run for a physical time span of over 90 s to ensure a steady equilibrium flow and the conservation of mass was achieved between inlet and outlet. The computation time for a complete run was approximately 12-24 hours on the workstation.

### Numerical model results and validation

The numerical results were validated systematically against experimental measurements conducted using the same flow conditions. Figure 3 shows the comparison between the numerically simulated free-surface elevation against the experimental measurements.

The results demonstrated a very good agreement between the 1D numerical, CFD and experimental data in terms of free-surface elevation throughout the culvert channel. The key was to use a realistic tailwater depth  $d_{\text{out}}$ . The CFD model used a pressure outlet, which was very sensitive to the prescribed free-surface level at the outlet. Herein, experimentally measured values were used at the outlet boundary to prescribe the tailwater depth, which was considered very important in reproducing the correct free-surface profile.

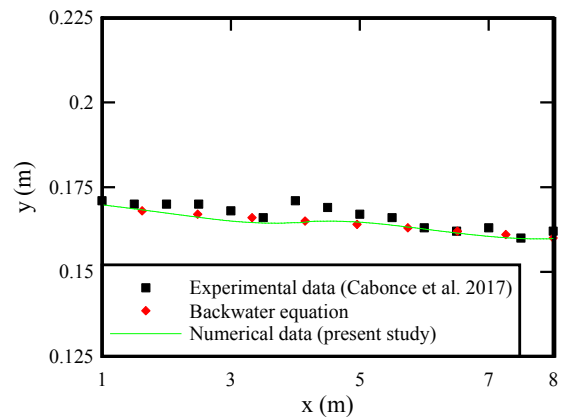


Figure 3. Free-surface comparison between 1D numerical, CFD and experimental results; experimental data from Cabonce et al. (2017); flow condition:  $Q = 0.056 \text{ m}^3/\text{s}$ ,  $d_{\text{out}} = 0.16$  m, channel with zero slope.

The vertical profiles of the longitudinal velocity at different transverse location, obtained from the numerical models, were compared to experimental results for validation purpose. Typical outcomes are presented in Figure 4. Overall, the CFD data compared favourably to experimental results for all transverse locations, with the locations near the sidewalls ( $z = 0.08$  m and  $0.42$  m) being better modelled than the centre of the channel. The results showed an overall tendency of over-estimating longitudinal velocity magnitudes for the CFD numerical model, especially towards the centreline of the channel. The maximum longitudinal velocity was over-estimated by 10% using the numerical model, compared to the experimental data (Fig. 4b).

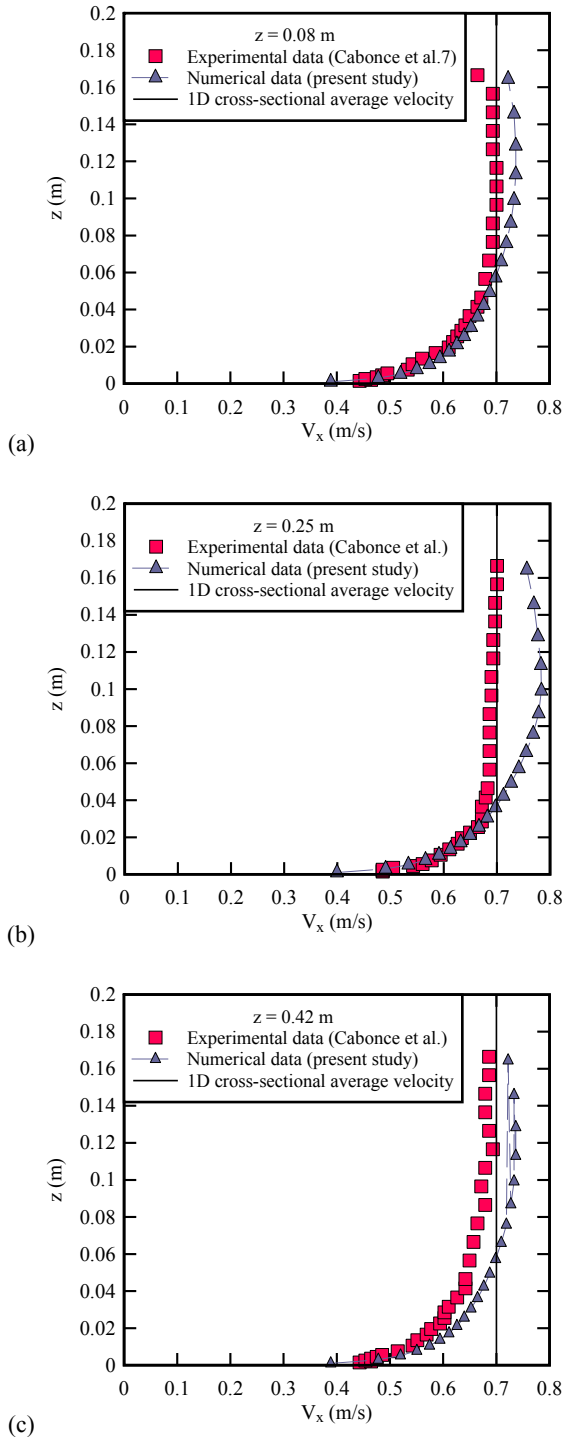


Figure 4. Longitudinal velocity comparison between 1D numerical, CFD and physical data; experiments by Cabonce et al. (2017); flow

conditions:  $Q = 0.056 \text{ m}^3/\text{s}$ ,  $d_{\text{out}} = 0.16 \text{ m}$ ,  $x = 7.5 \text{ m}$ , channel with zero slope; (a)  $z = 0.08 \text{ m}$ ; (b)  $z = 0.25 \text{ m}$  (centreline); (c)  $z = 0.42 \text{ m}$ .

Figure 5 shows typical longitudinal velocity contour in the  $y$ - $z$  plane, extracted at  $x = 7.5 \text{ m}$ , simulated by the numerical CFD model. Herein,  $x$  was measured from the start of the  $8 \text{ m}$  culvert barrel (Fig. 2). The velocity contour data showed similar range in velocity magnitude, compared to the experimental results of Cabonce et al. (2017). The shape of the contour and the boundary layer thickness along the bed and sidewalls were close to the physical measurements.

In the design of a fish-friendly culvert, the identification of the low-velocity zone is key. Typical small-bodied Australian fish swim at a characteristic speed less than  $0.5 \text{ m/s}$ . The contour line corresponding to this speed is highlighted by a white dashed line in Figure 5. Herein, the percentage of flow areas under different velocity values was calculated from the velocity contour data. Figure 6 shows the area fraction of longitudinal velocity under a certain relative velocity magnitude on the  $y$ - $z$  plane at  $x = 7.5 \text{ m}$ , with comparison to past CFD (Zhang and Chanson 2018) and physical data (Cabonce et al. 2017). The roughness of all CFD data was  $k_s = 0 \text{ m}$ , i.e. smooth boundaries. The results showed a good agreement between present and past numerical studies, despite differences in the model configurations. The model of Zhang and Chanson (2018) used a coupled solver and the top boundary was configured as symmetry rather than wall. Compared to the physical data, both numerical models tended to over-estimate the velocity magnitudes, yielding a reduced area of low velocity. However, this would result in a conservative estimation of the low-velocity zone, hence in a safer design.

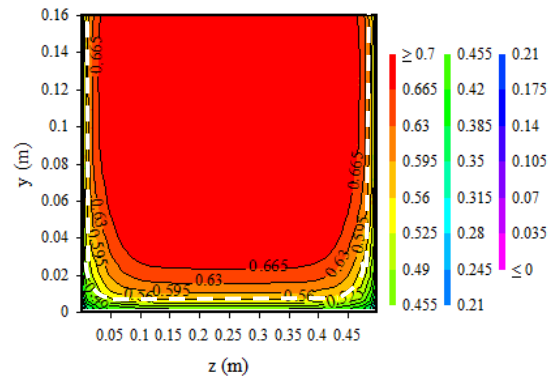


Figure 5. Longitudinal velocity contour in the  $y$ - $z$  plane at cross-section  $x = 7.5 \text{ m}$ ; flow condition:  $Q = 0.056 \text{ m}^3/\text{s}$ ,  $d_{\text{out}} = 0.16 \text{ m}$ ,  $x = 7.5 \text{ m}$ , channel with zero slope.

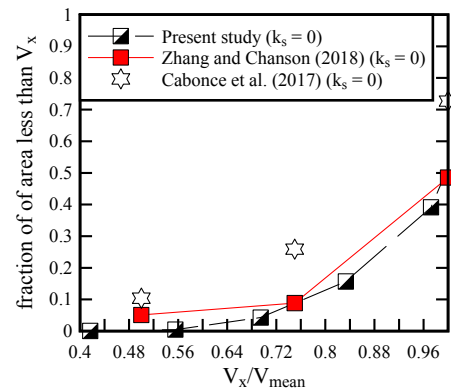


Figure 6. Percentage of area under different relative longitudinal velocity magnitude: comparison between present CFD data, past CFD

study (Zhang and Chanson 2018) and experimental study (Cabonce et al. 2017); flow condition:  $Q = 0.056 \text{ m}^3/\text{s}$ ,  $d_{\text{out}} = 0.16 \text{ m}$ ,  $x = 7.5 \text{ m}$ , channel with zero slope.

## Discussion

During the numerical investigation, a number of parameters were found to be of extreme importance in simulating the flow through a culvert barrel. One parameter was the tailwater level. It is vital to select a realistic tailwater level, if a realistic free-surface profile is to be produced. The present study used transient simulations for all models and all steps, and the results showed stable model performances. Although flows through the culvert could be treated as steady equilibrium flows in a long term, a steady flow simulation may not be the most appropriate approach due to the complexity of the coupling between free-surface and velocity profiles.

## Conclusion

A culvert is a common civil engineering structure installed under road embankment to pass through flood water. The ecological impact of a culvert has become important in recent years, namely the ability of the culvert to pass small-body-mass fish. The present study developed a numerical CFD approach to assist with the design fish-friendly culverts, through a three-dimensional modelling of the culvert barrel flow. The numerical results were systematically validated against detailed physical data for the same flow conditions and channel dimensions. The validation showed a good agreement between numerical and physical data, in terms of the free-surface and velocity profiles. The low-velocity zones were clearly identified and compared to experimental findings. The CFD data showed a conservative estimate of low-velocity zone size.

Overall, the present study showed the capacity of using a CFD model to predict the three-dimensional flow field in a culvert barrel, which could be used to design a fish-friendly culvert. The systematic validation against physical data is uppermost critical to ascertain the performances of a numerical model, and can be sensitive to a range of inflow conditions, boundary parameters, and the grid mesh quality and size.

## Acknowledgments

The authors thank Dr Matthew Gordos and Marcus Riches (NSW DPI Fisheries), and Professor Colin J. Apelt (The University of Queensland) for very helpful discussions. The financial support of Australian Research Council (Grant LP140100225) is acknowledged.

## References

- [1] Apelt, C.J. (1983). Hydraulics of Minimum Energy Culverts and Bridge Waterways. *Australian Civil Engineering Transactions*, Institution of Engineers, Australia, Vol. CE25, No. 2, pp. 89-95.
- [2] Behlke, C.E., Kane, D.L., McLeen, R.F., and Travis, M.T. (1991). Fundamentals of Culvert Design for Passage of Weak-Swimming Fish. *Report FHW A-AK-RD-90-10*, Department of Transportation and Public Facilities, State of Alaska, Fairbanks, USA, 178 pages.
- [3] Cabonce, J., Fernando, R., Wang, H., & Chanson, H. (2017). Using Triangular Baffles to Facilitate Upstream Fish Passage in Box Culverts: Physical Modelling. *Hydraulic Model Report No. CH107/17*, School of Civil Engineering, The University of Queensland, Brisbane, Australia, 130 pages.
- [4] Cabonce, J., Fernando, R., Wang, H., and Chanson, H. (2018). Using Small Triangular Baffles to Facilitate Upstream Fish Passage in Standard Box Culverts. *Environmental Fluid Mechanics*, Vol. 18 (DOI: 10.1007/s10652-018-9604-x).
- [5] Chanson, H. (2000). Introducing Originality and Innovation in Engineering Teaching: the Hydraulic Design of Culverts. *European Journal of Engineering Education*, Vol. 25, No. 4, pp. 377-391.
- [6] Chanson, H. (2004). *The Hydraulics of Open Channel Flow: An Introduction*. Butterworth-Heinemann, 2nd edition, Oxford, UK, 630 pages.
- [7] Fairfull, S., and Witheridge, G. (2003). Why do fish need to cross the road? Fish passage requirements for waterway crossings. *NSW Fisheries*, Cronulla NSW, Australia, 14 pages.
- [8] Henderson, F.M. (1966). *Open Channel Flow*. MacMillan Company, New York, USA.
- [9] Herr, L.A., and Bossy, H.G. (1965). Capacity Charts for the Hydraulic Design of Highway Culverts. *Hydraulic Eng. Circular*, US Dept. of Transportation, Federal Highway Admin., HEC No. 10, March.
- [10] Hirt, C., and Nichols, B. (1981). Volume of Fluid (VOF) method for the dynamics of free boundaries. *Journal of Computational Physics*, Vol. 39, No. 1, pp. 201-225.
- [11] Liggett, J.A. (1994). *Fluid Mechanics*. McGraw-Hill, New York, USA.
- [12] Moore, M., McCann, J., and Power, T. (2018). Greater Brisbane Fish Barrier Prioritisation. *Catchment Solutions Report*, 97 pages.
- [13] Olsen, A. and Tullis, B. (2013). Laboratory Study of Fish Passage and Discharge Capacity in Slip-Lined, Baffled Culverts. *Journal of Hydraulic Engineering*, ASCE, Vol. 139, No. 4, pp. 424-432.
- [14] Quadrio, J. (2007). Passage of Fish Through Drainage Structures. *Queensland Roads*, Sept., pp. 6-17.
- [15] Wang, H., and Chanson, H. (2018). Modelling Upstream Fish Passage in Standard Box Culverts: Interplay between Turbulence, Fish Kinematics, and Energetics. *River Research and Applications*, Vol. 34, No. 3, pp.244-252 (DOI: 10.1002/rra.3245).
- [16] Wang, H., Chanson, H., Kern, P., and Franklin, C. (2016). Culvert Hydrodynamics to enhance Upstream Fish Passage: Fish Response to Turbulence. *Proceedings of 20th Australasian Fluid Mechanics Conference*, Australasian Fluid Mechanics Society, Perth WA, Australia, 5-8 December, Paper 682, 4 pages.
- [17] Warren, M.L., Jr., and Pardew, M.G. (1998). Road crossings as barriers to small-stream fish movement. *Transactions of the American Fisheries Society*, Vol. 127, pp. 637-644.
- [18] Zhang, G., and Chanson, H. (2018). Three-dimensional numerical simulations of smooth, asymmetrically roughened, and baffled culverts for upstream passage of small-bodied fish. *River Research & Applications* Vol. 34, No. 8, pp. 957-964 (DOI: 10.1002/rra.3346).